

Screening of Photocatalysts by Scanning Electrochemical Microscopy

Joowook Lee, Heechang Ye, Shanlin Pan, and Allen J. Bard*

Center for Electrochemistry, Department of Chemistry and Biochemistry, The University of Texas at Austin, Austin, Texas 78712

A method for rapid screening of photocatalysts employing a form of scanning electrochemical microscopy (SECM) is described. A piezoelectric dispenser was used to deposit arrays composed of ~300- μm -size photocatalyst spots with different compositions onto conducting glass, fluorine-doped tin oxide substrate. The scanning tip of the SECM was replaced by a fiber optic connected to a xenon lamp and was rapidly scanned over the array. In this arrangement, the photocatalytic performance of the spots was evaluated by measuring the photocurrent at the substrate of the array. A fiber optic with a ring electrode can also be used to electrochemically detect products of the photoreaction. Several iron oxide-based bimetallic oxide combinations were found to exhibit enhanced photocatalytic activity, when compared to pure $\alpha\text{-Fe}_2\text{O}_3$. These combinations included iron–palladium, iron–europium, and iron–rubidium in specific ratios. A trimetallic bismuth–vanadium–zinc oxide combination was also found to show a higher photocurrent, by ~40%, compared to BiVO_3 .

Photoelectrochemical (PEC) systems based on semiconductor electrodes have shown the best efficiencies of chemical systems for the conversion of solar energy to electricity or fuels and have been extensively investigated. For example, the photoelectrolysis of water has been proposed as a means of using sunlight to produce hydrogen for use as a fuel. Such a PEC system, if inexpensive, efficient, and stable, would provide a practical method of producing high-purity hydrogen using an abundant energy source (sunlight), and water, and this “holy grail” has been sought for more than 35 years.¹ The first PEC system for the photoelectrolysis of water was described by Fujishima and Honda,² where a UV light-illuminated TiO_2 electrode immersed in an alkaline aqueous electrolyte was coupled to a Pt electrode in an acidic electrolyte to produce oxygen and hydrogen. Additionally a large number of PEC photovoltaic cells have been described. While progress has been made in our understanding of PEC systems, practical, inexpensive, efficient, and stable devices have not yet been attained. A PEC system utilizes a semiconductor electrode as the photoanode or photocathode. The electrode material for PEC application should have the following characteristics: (a) stability in aqueous electrolytes under solar illumination and (b)

a band gap of 1.3–1.4 eV for maximum incident sunlight absorbance. Additionally, for photoelectrolysis of water (c) a conduction band energy negative of the potential for water reduction and (d) a valence band energy positive of the potential for water oxidation are needed. In fact, the latter photocatalyst will almost certainly require a larger band gap than given in (b) (e.g., ~1.8 eV) with the use of electrocatalysts that promote proton reduction and water oxidation at reasonable overpotentials. Such a material may well be a combined bimetallic, trimetallic, or even higher compound, e.g., in the form of a chalcogenide. For example, in recent years modified semiconductors, such as modifications (by addition of dopants) of TiO_2 ,^{3–5} $\alpha\text{-Fe}_2\text{O}_3$,^{6,7} WO_3 ,⁸ and nanoparticle-imbedded TiO_2 ,⁹ have been investigated. More complex metal/element combinations have also yielded interesting semiconductors.^{10,11} However, the number of dopants and metal combinations that can be synthesized and tested is astronomical, and fast synthesis and testing methods are needed to screen through the candidate materials.

Combinatorial chemistry provides a rapid and systematic synthesis and screening method for a large number of materials with the preparation of different compositions. Such methods have been used, for example, in the search for new phosphors,^{12,13} sensors,¹⁴ and fuel cell catalysts.^{15,16} Several groups have employed combinatorial methods for photocatalysts. Woodhouse et

- (3) Park, J. H.; Kim, S.; Bard, A. J. *Nano Lett.* 2006, 6, 24.
(4) Irie, H.; Watanabe, Y.; Hashimoto, K. *J. Phys. Chem. B* 2003, 107, 5483.
(5) Asahi, R.; Morikawa, T.; Ohwaki, T.; Aoki, K.; Taga, Y. *Science* 2001, 293, 269.
(6) Ingler, W. B.; Khan, S. U. M. *Int. J. Hydrogen Energy* 2005, 30, 821.
(7) Sartoretti, C. J.; Alexander, B. D.; Solarska, R.; Rutkowska, I. A.; Augustynski, J.; Cerny, R. *J. Phys. Chem. B* 2005, 109, 13685.
(8) Hwang, D. W.; Kim, J.; Park, T. J.; Lee, J. S. *Catal. Lett.* 2002, 80, 53.
(9) Macak, J. M.; Barczuk, P. J.; Tsuchiya, H.; Nowakowska, M. Z.; Ghicov, A.; Chojak, M.; Bauer, S.; Virtanen, S.; Kulesza, P. J.; Schmuki, P. *Electrochim. Commun.* 2005, 7, 1417.
(10) Maeda, K.; Takata, T.; Hara, M.; Saito, N.; Inoue, Y.; Kabayashi, H.; Domen, K. *J. Am. Chem. Soc. Commun.* 2005, 127, 8286.
(11) Lu, D.; Takata, T.; Saito, N.; Inoue, Y.; Domen, K. *Nature* 2006, 440, 295.
(12) Danielson, E. D.; Devenney, M.; Giaquinta, D. M.; Golden, J. H.; Haushalter, R. C.; McFarland, E. W.; Poojary, D. M.; Reaves, C. M.; Weinberg, W. H.; Wu, X. D. *Science* 1998, 279, 837.
(13) Wang, J.; Yoo, Y.; Gao, C.; Takeuchi, I.; Sun, X.; Chang, H.; Xiang, X.-D.; Schultz, P. G. *Science* 1998, 279, 1712.
(14) Dickinson, T. A.; Walt, D. R.; White, J.; Kauer, J. S. *Anal. Chem.* 1997, 69, 3413.
(15) Cong, P.; Doolen, R. D.; Fan, Q.; Giaquinta, D. M.; Guan, S.; McFarland, E. W.; Poojary, D.; Self, K.; Turner, H. W.; Weinberg, W. H. *Angew. Chem., Int. Ed.* 1999, 38, 484.
(16) Reddington, E.; Sapienza, A.; Gurau, B.; Viswanathan, R.; Sarangapani, S.; Smotkin, E. S.; Mallouk, T. E. *Science* 1998, 280, 1735.

* To whom correspondence should be addressed. E-mail: ajbard@mail.utexas.edu.

(1) Bard, A. J.; Fox, M. A. *Acc. Chem. Res.* 1995, 28, 141.
(2) Fujishima, A.; Honda, K. *Nature* 1972, 238, 37.

al.^{17,18} used inkjet printing technology to print bimetallic and trimetallic photocatalysts and compared their photocatalytic performance to monometallic semiconductors. The McFarland group^{19,20} employed a robotic XYZ positioner to position a counter and reference electrode over an array of ~1-cm-diameter wells on an F-doped tin oxide (FTO) substrate-containing electrolyte and electrodepositing metal oxides (modified WO₃ or ZnO). These were tested for photoelectrochemical activity by scanning an optical fiber over each well. Our group has successfully employed SECM for rapid screening of bimetallic and trimetallic electrocatalysts for oxygen reduction and several useful electrocatalysts, e.g., based on Pd–Co, were found that showed activity in strong acid comparable to Pt.^{21,22} We describe here a modified form of this technique as applied to photocatalysts. In this technique, arrays of photocatalysts are prepared from drop coating an FTO substrate with solutions using an automated dispenser, as used with electrocatalysts, followed by suitable treatment to convert the spots to the desired oxide. In screening, the ultramicroelectrode tip is replaced by an optical fiber connected to a Xe light source, which illuminates each photocatalyst spot, and its photoactivity is determined from the photocurrent generated. A similar (metal-coated) fiber optic was used previously by our own group,²³ and also by the Smyrl group,^{24,25} for imaging purposes. Either a bare optical fiber or a metal-coated one to provide a ring electrode as part of the SECM tip can be used. In previous SECM studies of semiconductor materials, e.g., CdS²⁶ or TiO₂,²⁷ only a single large-area film was illuminated.

EXPERIMENTAL SECTION

Chemicals. FTO-coated glass was obtained from Pilkington (Toledo, OH). The 15 × 15 mm squares were cleaned by successive sonication in ethanol and 2-propanol and rinsed with deionized water. Fe(NO₃)₃·9H₂O (Baker), (NH₄)₃PdCl₄, RbCl, EuCl₃, Bi(NO₃)₃·6H₂O, NH₄VO₃, Na₂SO₄, Na₂SO₃, K₄Fe(CN)₆ (Aldrich), Ni(NO₃)₂·6H₂O (MCB), KOH, NaOH, H₂SO₄, ethylene glycol, glycerol (Fisher), and K₂PtCl₄ (Alfa Aesar) were used as received and Milli-Q water was used to prepare all solutions. All metal precursor solutions were made with either a 3:1 solution of water/glycerol (iron-based oxides) or ethylene glycol (bismuth-based oxides) with a metal salt concentration of 0.1 M.

Preparation of Photocatalyst Arrays. A CH Instruments model 1550 dispenser (Austin, TX) used to fabricate the photocatalyst arrays consists of a stepper-motor-operated XYZ stage

- (17) Woodhouse, M.; Herman, G. S.; Parkinson, B. A. *Chem. Mater.* **2005**, *17*, 4318.
- (18) Woodhouse, M.; Parkinson, B. A. *Chem. Mater.* **2008**, *20*, 2495.
- (19) Baeck, S. H.; Jaramillo, T. F.; Brändli, C.; McFarland, E. W. *J. Comb. Chem.* **2002**, *4*, 563.
- (20) Jaramillo, T. F.; Baeck, S. H.; Kleiman-Schwarzstein, A.; Choi, K. S.; Stucky, G. D.; McFarland, E. W. *J. Comb. Chem.* **2005**, *7*, 264.
- (21) Fernández, J. L.; Walsh, D. A.; Bard, A. J. *J. Am. Chem. Soc.* **2005**, *127*, 357.
- (22) Walsh, D. A.; Fernández, J. L.; Bard, A. J. *J. Electrochem. Soc.* **2006**, *153*, E99.
- (23) Lee, Y.; Ding, Z.; Bard, A. J. *Anal. Chem.* **2002**, *74*, 3634.
- (24) Casillas, N.; James, P.; Smyrl, W. H. *J. Electrochem. Soc.* **1995**, *142*, L16.
- (25) James, P.; Casillas, N.; Smyrl, W. H. *J. Electrochem. Soc.* **1996**, *143*, 3853.
- (26) Haram, S.; Bard, A. J. *J. Phys. Chem. B* **2001**, *105*, 8192.
- (27) Kemp, T. J.; Unwin, P. R.; Vincze, L. *J. Chem. Soc. Faraday Trans.* **1995**, *91*, 3893.
- (28) Bard, A. J.; Mirkin, M. V. *Scanning Electrochemical Microscopy*; Marcel Dekker: New York, 2001.

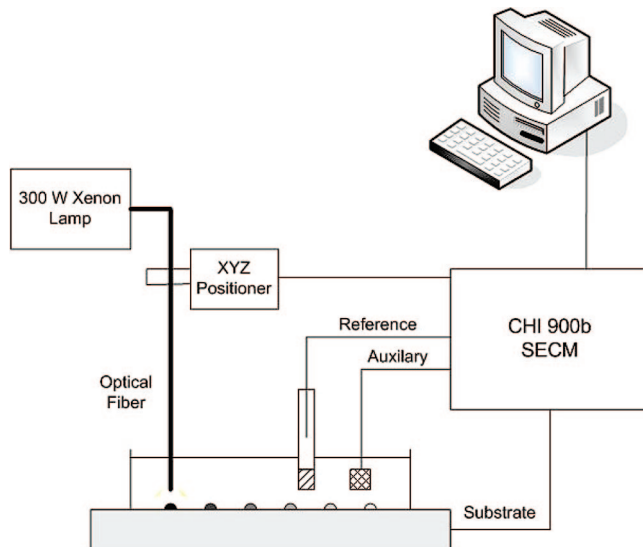


Figure 1. Schematic diagram of the setup for SECM measurements of PEC reactions under illumination.

with a piezodispenser (MicroJet AB-01-60, MicroFab, Plano, TX) attached to the head. The system was connected and controlled through a PC computer. The substrate (FTO) was placed under the piezodispenser tip and the XYZ stage moved the dispenser head in a preprogrammed pattern, while programmed voltage pulses were applied to the dispenser to eject the requested number of drops (~100 pL each) of the metal precursor solution onto the substrate. The first component (metal precursor solution) was loaded and dispensed in a preprogrammed pattern onto the FTO substrate. After flushing and washing the piezodispenser, the second component was loaded into the dispenser and dispensed into the existing pattern. The step was repeated when a third component was added. The relative number of drops of each component (~10 total) determined the spot composition. The metal component solutions that comprised the spots were mixed with a Vortex Genie 2 (Fisher, Pittsburgh, PA). The iron oxide arrays were annealed at 450 °C for 5 h, while the bismuth oxide arrays were annealed at 500 °C for 3 h.

Screening the Array. Figure 1 is a schematic diagram of the SECM setup. A 400-μm optical fiber (FT-400-URT, 3M, St. Paul, MN) connected to a 150-W xenon lamp was attached to the tip holder of a CHI model 900B SECM. The fiber was coupled to the Xe lamp via a model 9091 five-axis fiber aligner (New Focus, San Jose, CA). The array was placed in a SECM cell made of Teflon with the FTO/photocatalyst working electrode exposed at the bottom through an O-ring. A Pt wire counter electrode and Ag/AgCl reference electrode was used to complete the three-electrode configuration. Either 1 M KOH or 0.1 M Na₂SO₄ with 10 mM Na₂SO₃ as a sacrificial electron donor was used as the electrolyte. The optical fiber was positioned perpendicular to the working electrode surface and scanned across the surface at 500 or 300 μm/s (SECM setting 50 or 30 μm/0.1 s). A 420 nm long-pass filter was used in visible light illumination experiments. The optical fiber tip was held and scanned 50 μm above the working electrode surface, while a given potential was applied to the working electrode array by the SECM potentiostat. The photocurrent produced during the scan was measured and recorded to produce a color-coded two-dimensional image.

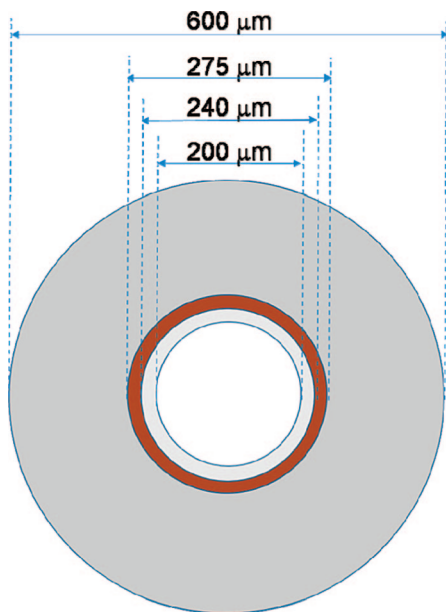


Figure 2. Schematic diagram of Au ring optical fiber (bottom view).

Au Ring Optical Fiber. For the detection of products, a commercial Au-coated optical fiber (Fiberguide Industries, Inc., Stirling, NJ) was used and sealed in a borosilicate glass capillary with heating under vacuum. The sealing procedure was the same as that used in the preparation of ultramicroelectrodes for normal SECM experiments described in ref 28. The resulting optical fiber had a Au ring electrode surrounded by a glass insulator. The dimensions of the Au ring optical fiber used were as follows: core diameter (d) of the optical fiber 200 μm ; inner d of the Au ring 240 μm ; outer d of the Au ring 275 μm ; d of the whole optical fiber including the glass insulator part 600 μm (Figure 2). The 20 mM $\text{K}_4\text{Fe}(\text{CN})_6$ in 0.1 M Na_2SO_4 aqueous solution was used in testing such tips. For detection of oxygen produced during the photooxidation of water at a BiVO_4 array, the Au ring electrode was electrochemically plated with Pt by applying 0.1 V (vs Ag/AgCl) for 300 s in 1.0 mM K_2PtCl_4 in 0.1 M H_2SO_4 aqueous solution.

X-ray Diffraction. X-ray diffraction (XRD) measurements were carried with a Bruker-Norius D8 advanced diffractometer. The $\text{Cu K}\alpha$ radiation source was operated at 40 kV and 40 mA. All measurements were carried out in the $\theta/2\theta$ mode. The 2θ scan data were collected using a scintillation detector at 0.01° intervals over the range 15°–70° and a scan rate of 3°/s. Samples for XRD analysis were prepared using the same metal salt solutions used to fabricate the photocatalyst arrays. The solutions were mixed according to the ratio determined by SECM experiments and spread out on a glass slide. They were then heated at the appropriate temperature. The resulting catalyst was scratched off the glass slide and packed into a powder XRD sample holder.

RESULTS AND DISCUSSION

Modified Fe_2O_3 Studies. Fe_2O_3 is a well-known photocatalyst that can be easily produced and modified, and has been the subject of many studies,^{17,29–31} and is a good candidate for modification with other metals. Arrays of Fe_2O_3 with different concentrations

of various second metals (dopants) (0–100% dopant in 10% increments) were fabricated and screened. XRD patterns (see the Supporting Information) verified that the phase of iron oxide formed via pyrolysis of iron(III) nitrate is $\alpha\text{-Fe}_2\text{O}_3$ (hematite).

Figure 3a shows the array pattern. The first and fourth rows were 100% Fe_2O_3 (10 drops of $\text{Fe}(\text{NO}_3)_3$) and were used as an internal standard and to assist in adjusting tilt of the sample stage. The SECM sample stage was adjusted until all spots of rows 1 and 4 displayed the same photocurrent value during a scan of the tip over the array. The numbers inside the circles represent the number of drops dispensed for that spot. The first and second numbers represent the number of drops of solutions of the first ($\text{Fe}(\text{NO}_3)_3$) and second component, respectively. Figure 3b shows the image obtained for a photocatalyst array consisting of Fe and Pd (only rows 2 and 3 are shown). The applied potential was 0.2 V versus Ag/AgCl, and the solution was 1 M KOH. An increase in the anodic photocurrent occurs with the addition of Pd, with a maximum at the Fe 70/Pd 30 spot (the number values represent the atom percent of the element based on the solution added). The maximum represents a 10% increase compared to pure Fe_2O_3 , i.e., pure Fe_2O_3 spot, 194 versus 220 nA, for a spots containing 30% Pd. When the amount of Pd became greater than 40%, the photocurrent dropped, probably because of the decrease in photoactive material (Fe_2O_3) in the spot and perhaps some quenching by the Pd. Photocurrents of spots containing 60% or more Pd become indistinguishable with the substrate current, and black outlines indicate the position of these spots in the figure. The same trend was seen at higher bias potentials (now shown). XRD patterns of Fe 70/Pd 30 photocatalysts (see the Supporting Information) reveal that the Pd is present in the Fe_2O_3 matrix in the form of Pd and PdO.

The addition of europium and rubidium to iron oxide also produced an enhancement in photocurrent. Figure 4a shows the SECM image of Fe/Eu photocatalyst arrays at 0.2 V versus Ag/AgCl. A 10% increase in photocurrent is observed at the Fe 90/Eu 10 spot. Higher concentrations of Eu show an adverse effect on the photocurrent, indicated by the drop in photocurrent at the Fe 80/Eu 20 spot and the spots thereafter. The photocurrent enhancement effect by the addition of Rb was greater than that seen with Pd or Eu. In Figure 4b, all spots containing 10–40% Rb showed a higher photocurrent compared to bare Fe_2O_3 . The enhancement reached a maximum at the Fe 80/Rb 20 spot, where the photocurrent was about double that of the Fe_2O_3 spot.

This technique is also able to identify elements that exhibit a negative effect on the photoelectrochemical response of Fe_2O_3 . Figure 5a displays the photocurrent response of the Fe/Co photocatalyst array. An immediate drop in photocurrent was observed beginning with the Fe 90/Co 10 spot. Ni also inhibited the photocatalytic activity (Figure 5b), but the effect of Ni was more gradual than that of Co. The photocurrent gradually decreased for Fe 90/Ni 10 and Fe 80/Ni 20 spots and then dropped below the substrate current after ~30% Ni was added.

Numerous papers have detailed the modification of iron oxide via doping with other metals.^{17,29–31} The purpose of our experiments using iron oxides was to prove the concept of rapid

(30) Sartoretti, C. J.; Alexander, B. D.; Solarska, R.; Rutkowska, I. A.; Augustynski, J.; Cerny, R. *J. Phys. Chem. B* **2005**, *109*, 13685.

(31) Cesar, I.; Kay, A.; Gonzalez Martinez, J. A.; Grätzel, M. *J. Am. Chem. Soc.* **2006**, *128*, 4582.

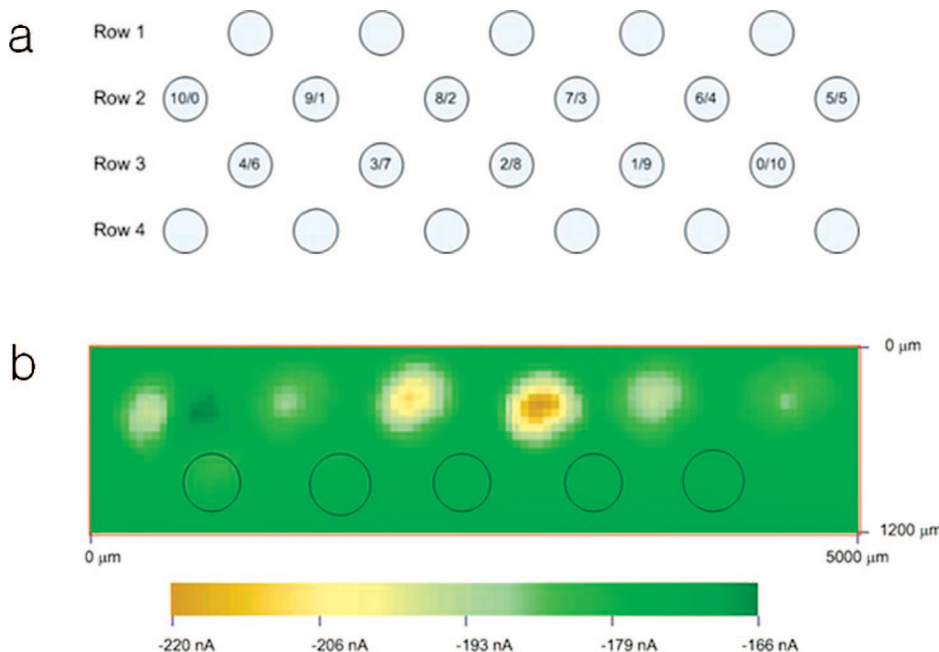


Figure 3. (a) Dispensed pattern of photocatalyst arrays. The first and fourth rows are 100% Fe_2O_3 . For rows 2 and 3, the first and second numbers inside each circle represent the number of drops of the first ($\text{Fe}(\text{NO}_3)_3$) and second component, respectively. (b) SECM image of Fe/Pd photocatalyst at applied potential of 0.2 V vs Ag/AgCl in 1 M KOH under UV-vis light illumination.

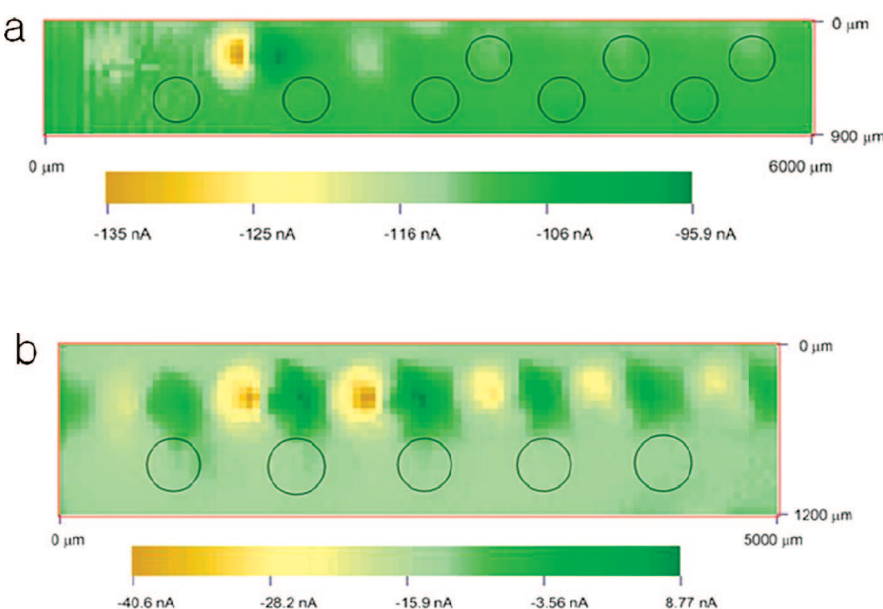


Figure 4. SECM images of (a) Fe/Eu photocatalyst and (b) Fe/Rb photocatalyst at applied potential of 0.2 V vs Ag/AgCl in 1 M KOH under UV-vis light illumination.

screening of photocatalysts with SECM, and Fe_2O_3 was chosen because it is a widely known modifiable photocatalyst. Further investigation into the mechanism by which each metal increases or decreases photocurrent was not considered in this study.

Systems Based on Bi–V–O. The photocatalytic properties of bismuth vanadate (BiVO_4) in the visible region, e.g., for oxygen evolution and organic pollutant degradation, makes this an interesting material for further study.^{32,33} Here we describe the use of SECM with the Bi–V–O system to investigate trimetallic

photocatalysts, e.g., for the addition of zinc into BiVO_4 . Bismuth–vanadium–zinc oxides were fabricated using $\text{Bi}(\text{NO}_3)_3$, NH_4VO_3 , and $\text{Zn}(\text{NO}_3)_2$ as the first, second, and third components in the dispenser, respectively. The array formed a triangle, with each corner composed of 100% (10 drops) of one compound. Figure 6 shows the SECM image of a Bi–V–Zn oxide array at 0.2 V versus Ag/AgCl in 0.1 M Na_2SO_4 with 10 mM Na_2SO_3 as a sacrificial electron donor under (a) UV-vis and (b) visible light illumination. The top corner represents 100% Bi–O, with the concentration decreasing by 10% for each adjacent row. The bottom left and bottom right corners are composed of 100% V–O and Zn–O, respectively. Their concentrations also decrease by 10% for each

(32) Tokunaga, S.; Kato, H.; Kudo, A. *Chem. Mater.* 2001, 13, 4624.

(33) Sayama, K.; Nomura, A.; Arai, T.; Sugita, T.; Abe, R.; Yanagida, M.; Oi, T.; Iwasaki, Y.; Abe, Y.; Sugihara, H. *J. Phys. Chem. B* 2006, 110, 11352.

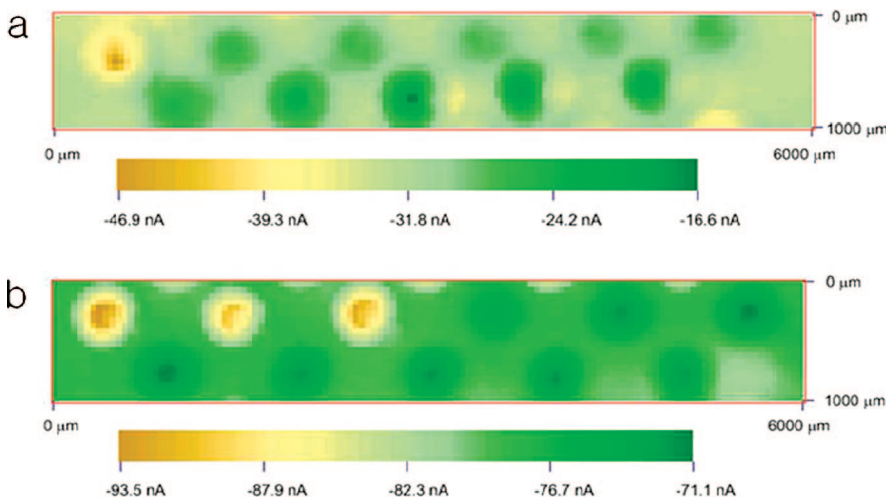


Figure 5. SECM images of (a) Fe/Co photocatalyst and (b) Fe/Ni photocatalyst at applied potential of 0.2 V vs Ag/AgCl in 1 M KOH under UV-vis light illumination.

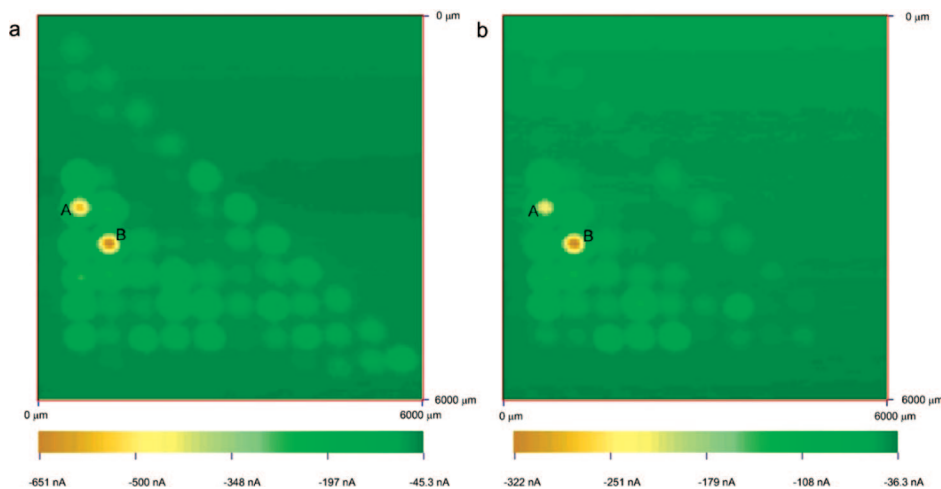


Figure 6. SECM images of Bi/V/Zn photocatalyst at 0.2 V vs Ag/AgCl applied potential under (a) UV-vis and (b) visible light (>420 nm) illumination. In the array, the upper corner is 100% Bi, the lower left corner is 100% V, and the lower right corner is 100% Zn. Spots A and B represent Bi/V/Zn of 50/50/0 and 45/50/10 atom %, respectively.

adjacent column. The array includes 66 different combinations of Bi–V–Zn oxide photocatalysts, and the SECM technique allows the rapid evaluation of the performance of all 66 spots in a matter of minutes. The left column is composed of Bi- and V-only combinations. Spot A in Figure 6a is composed of Bi50/V50, which is the most commonly used Bi/V ratio to form BiVO₄. The higher photocurrent compared to other Bi/V ratios indicated that 50:50 is the optimum ratio for BiVO₄. But the highest photocurrent in the array is achieved when 10% Zn is mixed into the BiVO₄. This combination (spot B) shows an 18% increase in photocurrent over bare BiVO₄. The increase is enhanced when only visible light is used to illuminate the photocatalysts, with spot B showing a 40% increase in photocurrent over the BiVO₄ (Figure 6b).

Detection of Products. To detect the products generated in the photoelectrochemical experiments, we introduced an Au ring electrode around the optical fiber as described in the Experimental Section. Using this Au ring optical fiber, we obtained SECM images on the BiVO₄ arrays with 20 mM K₄Fe(CN)₆ in 0.1 M Na₂SO₄ aqueous solutions. Figure 7 shows the SECM images of both substrate (a) and tip (b). The applied potentials were 0.1 and −0.2

V versus Ag/AgCl for the substrate and the tip, respectively. Here, Fe(II) is oxidized to Fe(III) on substrate under illumination, and the generated Fe(III) is reduced on the Au ring electrode. As a result, two separate images were obtained as Figure 7. In Figure 8, the illuminated light was blocked in the middle of the scanning process; this removed photocurrent from the spots and tips. This result confirms that the current with the round spot shape in the SECM images is generated by the light.

In addition, the photooxidation of water on the BiVO₄ spots was performed in 0.2 M NaOH solution, and the product (O₂) was electrochemically detected on the tip via the O₂ reduction reaction (ORR). In this case, a Pt ring electrode was used to carry out the ORR, since Pt is a good electrocatalyst for this reaction. Figure 9 shows SECM tip current images of the BiVO₄ array on the substrate held at 0.2 V with the tip at −0.4 V. The ability to observe products of the photoreaction should allow quantitative measurements in this substrate generation/tip collection mode, which is, however, a function of the size of the spot and the detecting tip. Simulations and applications of this mode are being contemplated.

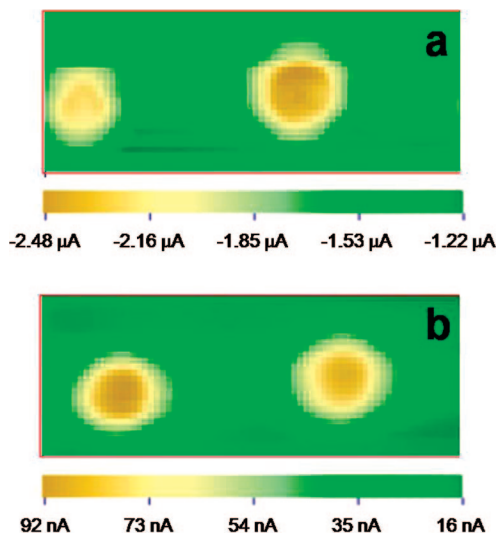


Figure 7. SECM images of BiVO_4 photocatalysts on the substrate at 0.1 V vs Ag/AgCl (a) and on the tip at -0.2 V vs Ag/AgCl (b) under UV-vis light illumination. Negative current shows anodic current and positive current, cathodic current. Both of the spots contain Bi and V in 1:1 ratio. Scan rate was 100 $\mu\text{m}/\text{s}$ (SECM setting 30 $\mu\text{m}/0.3$ s).

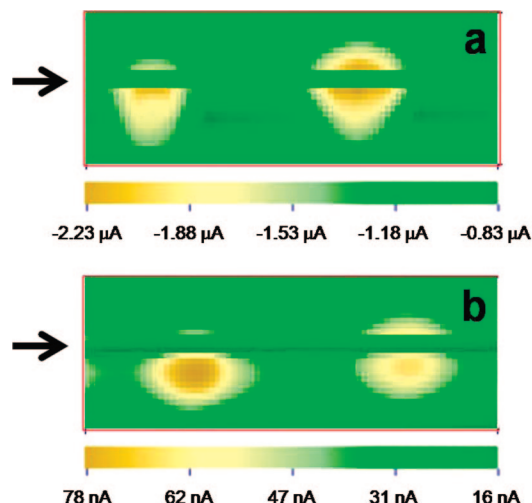


Figure 8. SECM images of BiVO_4 photocatalysts as in Figure 7 with light blocked during the middle of scan. Both of the spots contain Bi and V in 1:1 ratio. Scan rate was 100 $\mu\text{m}/\text{s}$ (SECM setting 30 $\mu\text{m}/0.3$ s).

CONCLUSIONS

We have introduced a new technique for rapid screening of photocatalysts that can quickly identify bimetallic and trimetallic combinations and their ratios which yield high photocatalytic effects based on modification of a commercial SECM. This technique not only allowed the identification of new dopants that enhanced photocurrent but also was used to confirm optimum

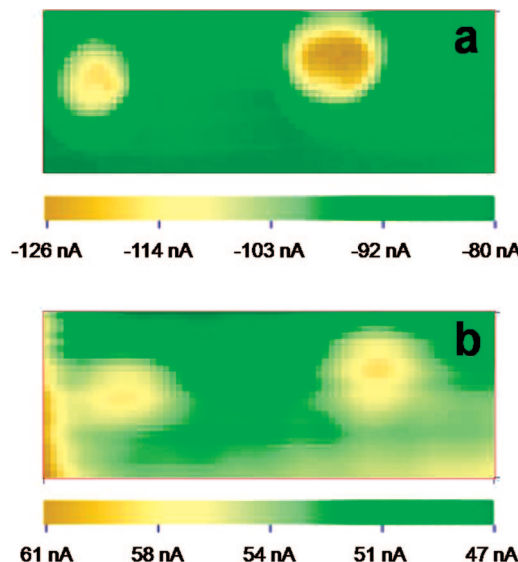


Figure 9. SECM images of BiVO_4 photocatalysts. (a) Substrate current and (b) tip current with substrate at 0.2 V vs Ag/AgCl and the tip at -0.4 V vs Ag/AgCl in Ar-saturated 0.2 M NaOH aqueous solution under UV-vis light illumination. The tip current is the reduction of oxygen generated on BiVO_4 spots photoelectrochemically. Scan rate was 100 $\mu\text{m}/\text{s}$ (SECM setting 30 $\mu\text{m}/0.3$ s).

metal ratios of known bimetallic oxide photocatalysts. The combination of a piezodispenser and SECM allowed for a quick, easy, and reproducible method of fabricating $\sim 300\text{-}\mu\text{m}$ -spot size photocatalyst arrays and a rapid and reliable method of evaluating their photocatalytic effects. The bimetallic and trimetallic combinations found in this study are currently being examined in detail through bulk studies, and we are searching for other high-performance photocatalysts.

Finally, the optical fiber modified with an Au or Pt ring and glass insulator allows products of the photoelectrochemical reaction to be detected electrochemically on the Au or Pt ring.

ACKNOWLEDGMENT

Fellowship support for J.L. was provided by the Korea Research Foundation Grant (KRF-2005-214-C00204). S.P. thanks the American Chemical Society for The Irving S. Sigal Fellowship. Support of this research by MERCK KGAA (UTA-07322), the Robert A. Welch Foundation (F-0021), and the National Science Foundation (CHE-0451494) is greatly appreciated.

SUPPORTING INFORMATION AVAILABLE

Additional information as noted in text. This material is available free of charge via the Internet at <http://pubs.acs.org>.

Received for review June 5, 2008. Accepted July 18, 2008.

AC801142G